Textile Research Journal | Article

An Application of Queuing Theory to Modeling of Melange Yarns Part I: A Queuing Model of Melange Yarn Structure

Abstract A queuing model of staple fiber yarn is presented that enables the modeling and a better understanding of fiber migration in a yarn. The model provides a fine yarn structure where the migrational behavior of fibers is associated with the behavior of customers traveling across an open network of queuing systems to get services. Based on this analogy, the underlying mathematical foundation of the queuing theory is used for the modeling of yarn structure and properties. The model uses yarn technical specifications including yarn linear density and twist level, fiber linear density and length distribution, together with specific parameters such as fiber packing density distribution and migration probabilities. The model can be used for modeling a wide range of structurally different yarns; examples include marl, mottle and melange yarns, yarns with different levels of hairiness, and yarns produced by various spinning systems. The model can be used for 3D simulation of yarns in computer-aided design systems for textile design and for the prediction of mechanical properties of yarns.

Key words fiber contact point, fiber migration, melange yarn, migration probability, queuing system

Francois Siewe[1] **and Sergei Grishanov**
TEAM Research Group, De Montfort University, Leicester, United Kingdom

Thomas Cassidy and Geoffrey Banyard
School of Design, University of Leeds, Leeds, United Kingdom

Yarn structure is one of the important characteristics which define yarn mechanical properties and appearance. For example, it is known that the mechanical properties of a ring-spun and an open-end spun yarn of the same linear density and produced from the same fibers are different [1, 2]. This is caused by the difference in their internal structure, which can be characterized by the cross-sectional and longitudinal distribution of fibers.

A staple fiber yarn is composed of short-length fibers which are assembled and twisted together. Fibers start at different distances from the beginning of the yarn. The radial positions of fibers within the yarn body change randomly (with *unknown* probability distribution) along the yarn axis. This behavior is known as *fiber migration*. Fiber migration is now a universally recognized phenomenon of yarn structure which provides necessary entanglement and cohesion between the fibers, thus creating a *continuous* structure devised from a *discrete* set of fibers. This dual nature of the structure of a staple fiber yarn makes it difficult to be modeled. Theoretical and experimental investigations of structure-properties relationship of yarns conducted over

[1] Corresponding author: TEAM Research Group, De Montfort University, Leicester, United Kingdom. e-mail: fsiewe@dmu.ac.uk

the last 50 years generally followed four main approaches towards modeling the fiber migration:

1. A deterministic approach based on the description of the geometry of individual fibers [3–8];
2. An approach based on the consideration of mechanical behavior of fibers [3, 8, 9];
3. A stochastic approach which describes internal yarn structure in terms of fiber packing density distribution over the yarn cross-section or fiber orientation distribution [10–14];
4. A combination of stochastic and mechanical approaches [13, 15].

These investigations mainly concerned the description of yarn structure and its effects on yarn mechanical properties. At the same time, spatial position of individual fibers in blended yarns has a dramatic effect on yarn appearance. For example, predominantly outward migration of flax fibers in flax-cotton blended yarn makes the yarn look as if it has been spun from 100 % flax fibers, although in fact a 30/70 % flax-cotton blend was used [16]. Similar effects can be seen in melange yarns where the overall color depends on the color of components, blend composition and spatial position of fibers.

Many existing computer-aided design systems provide textile technologists and designers with a facility to design yarns and fabrics in 3D. However, the images generated by such systems quite often suffer from an unrealistic representation of yarns because they model yarns as solid tubes lacking any fibrous structure. It is also difficult to obtain technical specification from such yarn images which would be useful to textile technologists. There have been very few attempts to generate realistic images of yarns on the basis of the above-mentioned models [14]. Better images could be generated if the yarn model was established on the basis of technical description of the yarn and provided means to determine the spatial disposition of individual fibers in the yarn structure.

Part I of this work presents a refined model of fiber migration in staple fiber yarns based on approaches previously reported [10, 12, 15] using a network of markovian queues. Basics of the queuing theory are introduced using Kendall's notation [17, 18]. The yarn structure is considered as divided into a number of cross-sections. Each cross-section is divided into concentric ring zones, which in turn consist of a fixed number of virtual locations [15]. Equations describing the behavior of fibers are generated using Erlang's and Little's formulae [17, 18]. The model enables important characteristics of yarn structure, such as the distribution and the average number of fibers in yarn cross-section, average yarn linear density, and average fiber packing fraction, to be predicted. A theoretical approach to the estimation of the number of contact points between the fibers has been proposed; this was based on a detailed consideration of the fiber neighborhood. In Part II, this model is used to generate an algorithm and software for the computer simulation and visualization of realistic 3D images of staple fiber yarns, including multi-component melange yarns. Part III will report the results of the experimental investigation of more than 100 different melange yarn samples and discuss the application of this model for the prediction of the color of melange yarns.

Basics of Queuing Theory

The queuing theory is a mathematical theory of waiting lines where customers queue to receive services. Typically, a queuing system has one service center and a waiting room (a queue) of finite or infinite capacity. The service center has one or more servers. Customers from a population or source enter a queuing system to receive some services. Upon arrival, a customer joins the waiting room if all servers in the service center are busy and waits until a server is available. When a customer has been served, he leaves the queuing system.

The behavior of a queuing system is characterized by the inter-arrival time distribution, A, the service time distribution, B, the number of servers, c, the system capacity, K (i.e. the number of servers plus the size of the waiting room), the population size, E, and the service discipline. The first five characteristics are generally denoted by the Kendall's notion $A/B/c/K/E$ [17, 18]. The symbols traditionally used for A and B are M (for exponential distribution), D (for deterministic distribution) and G or GI (for general distribution). A queuing system of infinite capacity (i.e. $K = \infty$) and infinite population size (i.e. $E = \infty$) is denoted as $A/B/c$. The service discipline defines the order in which customers are served such as First Come First Served (FCFS), Last Come First Served (LCFS) or Processor Sharing (PS).

This section briefly describes the $M/M/1$ queuing system and the Jackson network of such queuing systems.

The $M/M/1$ Queuing System

A $M/M/1$ queuing system has a single server and a waiting room of infinite capacity. The customers arrive independently according to a Poisson process with rate λ. The time it takes to serve every customer is exponentially distributed with parameter μ. The service times are supposed to be mutually independent and further independent of the inter-arrival times. The service discipline is FCFS. Because the inter-arrival times and the service times are exponentially distributed, the $M/M/1$ is a *markovian queue*.

At any point in time only one event occurs, with an event either being the arrival of a new customer or the completion of a customer's service. The system state is defined to be the number of customers in the system, i.e. the number of cus-

tomers being served and those waiting in the queue. Let $N(t)$ denote the state of the system at time $t \geq 0$. Let the quantity $\rho = \lambda/\mu$ be the *traffic intensity*, i.e. the mean quantity of work brought to the system per unit of time. It has been shown [17, 18] that the steady-state probability $\tau(n) = \lim_{t \to \infty} P\{N(t) = n\}$ of the system being in state n is defined by

$$\tau(n) = (1 - \rho)\rho^n, \tag{1}$$

provided that $\rho < 1$. In the case $\rho \geq 1$, the arrival rate λ is higher than or equal to the departure rate μ, and therefore the system will never reach a stationary state. Equation (1) states a time-independent probability density function of the number of customers in the system at steady-state.

The relationship between the average number of customers in the system, $\overline{N}$, and the average time a customer spends in the system, $\overline{T}$, is given by Little's law [17], viz.

$$\overline{N} = \lambda \overline{T}. \tag{2}$$

Jackson Open Network of *M*/*M*/1 Queuing Systems

A finite number of *M*/*M*/1 queuing systems can be interconnected into a network. One basic classification of queuing networks is the distinction between *open* and *closed* queuing networks. In an open network, new customers may arrive from outside the system (coming from a conceptually infinite population) and later on leave the system. In a closed network, the number of customers in the system is fixed and no customers enter or leave the system.

In this section, a Jackson open network consisting of m *M*/*M*/1 queuing systems is considered. The queues are numbered from 0 to $m - 1$. Customers arriving from outside the system join the queue i according to a Poisson process with rate λ_i^0. Having been served at queue i, where service time is exponentially distributed with parameter μ_i, the customer either leaves the system with probability p_i^0, or goes to queue j, with probability p_{ij}. The normalization condition holds for each queuing system in the network, viz.

$$\sum_{j=0}^{m-1} p_{ij} + p_i^0 = 1, \quad i = 0, \ldots, m-1. \tag{3}$$

The system state is a vector $(n_0, n_1, \ldots, n_{m-1})$, such that each component n_i is the number of customers in the queuing system i, $i = 0, \ldots, m-1$. It has been shown [17, 18] that the steady-state probability of the system being in state $(n_0, n_1, \ldots, n_{m-1})$ is defined by the product form

$$\delta(n_0, n_1, \ldots, n_{m-1}) = \tau_0(n_0) \cdot \tau_1(n_1) \cdot \ldots \cdot \tau_{m-1}(n_{m-1}) \tag{4}$$

where $\tau_i(n_i) = (1 - \rho_i)\rho_i^{n_i}$ is the steady-state probability of the queuing system i being in state n_i; $\rho_i = \lambda_i/\mu_i$ is the traffic intensity of the queuing system i.

The total arrival rate λ_i to the queuing system i is the *sum* of all arrivals to the queuing system i, viz.

$$\lambda_i = \lambda_i^0 + \sum_{j=0}^{m-1} p_{ji}\lambda_j, \quad i = 0, 1, \ldots, m-1. \tag{5}$$

Thus, the network behaves as if it were composed of independent *M*/*M*/1 queuing systems.

Modeling the Structure of Staple Fiber Yarns

Yarn Structure

Traditionally, the structure of a yarn is analyzed by observing successive cross-sections. Several approaches have been developed to model yarn cross-sections [1, 12, 15, 19]. In this paper, we assume the model described by Morris et al. and Grishanov et al. [12, 15], where a cross-section is modeled as a set of K concentric circular ring zones around the yarn center. The ring zones are assumed to have identical width $d = \overline{d}_f + \sigma_f$, where $\overline{d}_f$ and σ_f are the average and the standard deviation of the fibers' diameters, respectively. Each ring zone is divided into a fixed number of virtual locations (VLs) represented as circles of the same diameter d as shown in Figure 1(a). The ring zones are numbered from 0 to $K - 1$ starting from the yarn center towards the yarn surface. The ring zone 0 is situated at the yarn center and consists of exactly one VL. A ring zone i, $1 \leq i < K$, contains $\lfloor 2\pi i \rfloor$ (i.e. the greatest integer less than or equal to $2\pi i$) VLs. In this way, the ring zone 1 contains six VLs, the ring zone 2 contains 12, the ring zone 3 contains 18 and so on as depicted in Figure 1(b). The virtual locations of each zone i are numbered counter-clockwise from 0 to $\lfloor 2\pi i \rfloor - 1$ and the virtual location 0 is centered on the x-axis as illustrated in Figure 1(b). The virtual location r of the ring zone i is referred to by the pair (i, r).

Intuitively, a VL determines the radial and the angular position of the occupying fiber within the yarn cross-section. A virtual location accommodates at most one fiber at a time. Along the yarn body, a fiber may migrate from one VL to another with a probability p_{ij} (equation (3)). In the general case of all $p_{ij} \neq 0$ a customer can go to any queue j from any queue i (see Figure 2(a) showing a graph of transitions). However, in the case of application of queuing theory to modeling the fiber migration there are limitations imposed by layered yarn structure (Figure 2(b)). Since a fiber is a smooth body, it cannot migrate from a ring zone i into the ring zone $i + 2$ or $i - 2$ without first vis-

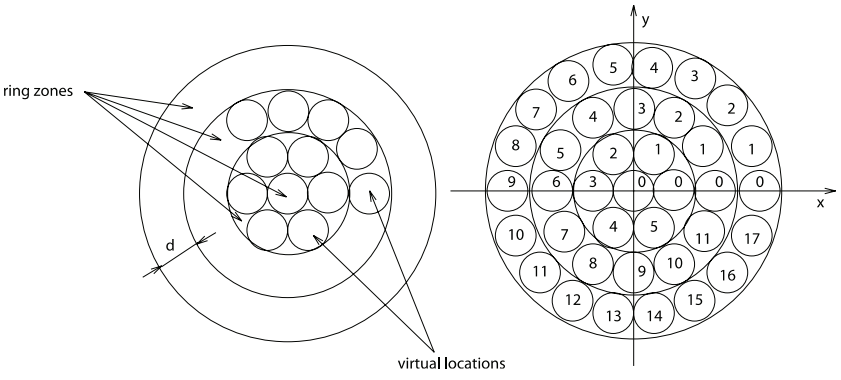

(a) Ring Zones and Virtual Locations (b) Numbering of Virtual Locations

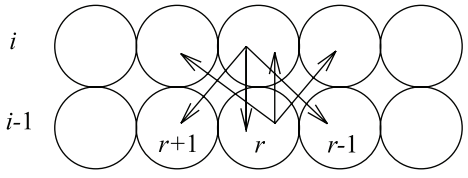

(c) Neighbouring Virtual Locations in the outermost zone of an infinitely large cross-section

Figure 1 A model of yarn cross-section.

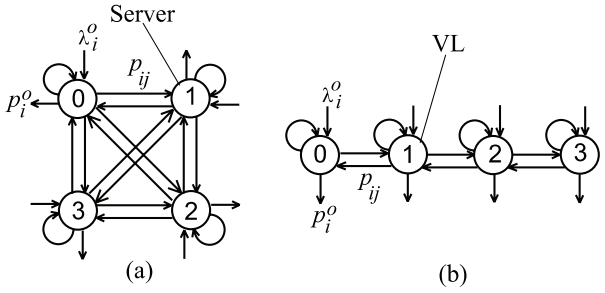

Figure 2 An open network of queuing systems with four servers (a) and a simple yarn model with a single VL in four ring zones (b).

iting the ring zone $i + 1$ or $i - 1$, respectively. This is illustrated in Figures 1(b) and 2(b), where it is clear that a fiber cannot migrate from a VL in the ring zone 1 to a VL in the ring zone 3 without first visiting a VL in the ring zone 2. This raises the necessity of defining which virtual locations are the closest neighbors to a virtual location in a yarn cross-section.

Definition 3.1 A virtual location is a closest neighbor of another virtual location if the segment of a straight line that joins their centers does not intersect a third virtual location.

Definition 3.2 An elementary migration action is taken when a fiber changes its position from one VL to a closest neighbor.

This yarn model allows only elementary migration actions. The probabilities p_{ij} for the virtual locations which are not the closest neighbors must be set to 0. Therefore, a fiber takes at least n steps to migrate from a virtual location in a ring zone i to a virtual location in the ring zone $i + n$, for some natural numbers i and n.

Computing the Closest Neighbors of a VL

Let $I_{i,r}$ denote the set of all closest neighbors of the virtual location (i, r) with respect to Definition 3.2. It follows from Definition 3.1 that the central virtual location of a yarn cross-section, i.e. the virtual location (0, 0), has six closest neighbors which are the six virtual locations of the ring zone 1, viz.

$$I_{0,0} = \{(1, 0), (1, 1), (1, 2), (1, 3), (1, 4), (1, 5)\}.$$

Each virtual location (i, r), $0 < i < K - 1$, has three closest neighbors in the ring zone $i + 1$ which are the virtual locations $(i + 1, f_0(i, r))$, $(i + 1, f_1(i, r))$ and $(i + 1, f_2(i, r))$ where

$$f_m(i, r) = \psi_{i+1}\left(m - 1 + \left\lfloor 0.5 + \left(\frac{2\pi(i+1)}{\lfloor 2\pi i \rfloor} r\right)\right\rfloor\right) \qquad (6)$$

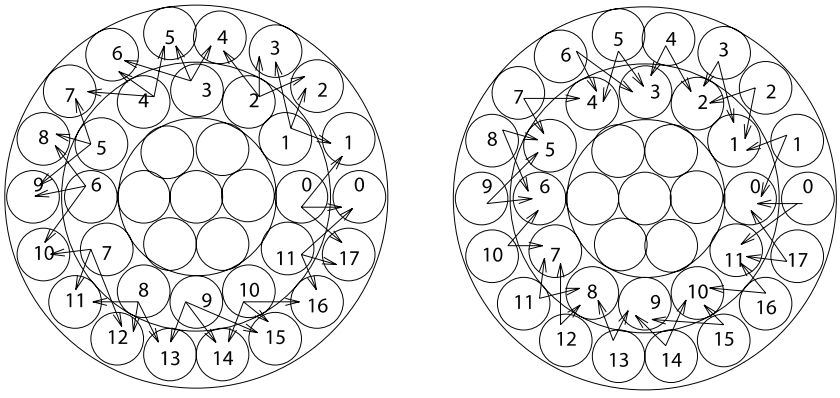

(a) (b)

Figure 3 Fiber migration directions.

Table 1 Neighborhood functions.

		VLs of the ring zone 2											
		0	**1**	**2**	**3**	**4**	**5**	**6**	**7**	**8**	**9**	**10**	**11**
VLs of the ring zone 3	f_0	17	1	2	4	5	7	8	10	11	13	14	16
	f_1	0	2	3	5	6	8	9	11	12	14	15	17
	f_2	1	3	4	6	7	9	10	12	13	15	16	0

for $m = 0, 1, 2$ and $\lfloor x \rfloor$ stands for the greatest integer less than or equal to x; the function $\psi(x)$ denotes the remainder of the division of x by $\lfloor i2\pi \rfloor$ and is defined for $i > 0$ as follows: $\psi_i(x) = x \bmod \lfloor 2\pi i \rfloor$. For example, the virtual location (2, 0) is a closest neighbor to the virtual locations (3, 0), (3, 1) and (3, 17) as shown in Figure 1(b). Table 1 gives the values of the functions f_m, $0 \le m \le 2$, for the 12 virtual locations of the ring zone number 2. This is illustrated graphically in Figure 3(a) where arrows originating from a virtual location in zone 2 point to the neighboring virtual locations in zone 3.

Because the closest neighbor relationship is symmetrical, each virtual location (i, r), $1 < i < K$, is a closest neighbor of the virtual location $(i - 1, r')$ of the ring zone $i - 1$, provided that $f_0(i - 1, r') = r$ or $f_1(i - 1, r') = r$ or $f_2(i - 1, r') = r$. For example, the virtual location (3, 0) is a closest neighbor to the virtual locations (2, 0) and (2, 11) as shown in Figure 1(b). This is illustrated graphically in Figure 3(b) where arrows originating from a virtual location in zone 3 point to the neighboring virtual locations in zone 2.

Let $\tilde{f}_m(i, r)$ denote the VL r' in the ring zone $i - 1$, if it exists, which is the closest neighbor to the VL r in zone i, i.e. $f_m(i - 1, r') = r$, for $1 < i < K$ and $m = 0, 1, 2$. Because a ring zone i contains more VLs than the ring zone $i - 1$, there may exist some VL (i, r) for which $\tilde{f}_0(i, r)$ does not exist, for some i, $1 < i < K$. Similar observations apply to $\tilde{f}_1(i, r)$ and $\tilde{f}_2(i, r)$. For example, in Table 1 it is clear that $\tilde{f}_0(3, 0)$, $\tilde{f}_1(3, 1)$ and $\tilde{f}_2(3, 2)$ do not exist. However, for each VL (i, r), at least one of the following neighboring VLs is defined for any ring zone $i \ge 1$: $\tilde{f}_0(i, r)$, $\tilde{f}_1(i, r)$ and $\tilde{f}_2(i, r)$. In the case of an infinitely large cross-section shown in Figure 1(c), each VL (i, r) in the outermost ring zone i has three neighbors $\tilde{f}_0(i, r)$, $\tilde{f}_1(i, r)$ and $\tilde{f}_2(i, r)$ in the ring zone $i - 1$. In the case of the ring zone 1, each VL has only one neighbor in the zone 0 which is $\tilde{f}_1(i, r) = (0, 0)$. Thus, all VLs in the zone $i \ge 1$ will have between 1 and 3 neighbors in the zone $i - 1$.

Furthermore, each virtual location (i, r) is a closest neighbor to its counter-clockwise successor $(i, \psi_i(r + 1))$ and its counter-clockwise predecessor $(i, \psi_i(r - 1))$. Where the function $\psi_i(x)$ denotes the remainder of the division of x by $\lfloor 2\pi i \rfloor$ and is defined for $i > 0$ as follows:

$$\psi_i(x) = x \, mod \lfloor 2\pi i \rfloor$$

For example, the virtual location $(2, \psi_2(4))$ is (2, 4), the virtual location $(2, \psi_2(12))$ is (2, 0) and the virtual location $(2, \psi_2(-1))$ is (2, 11), see Figure 1(b).

The closest neighborhood of a virtual location in the ring zone 1 is given by:

$$I_{1,r} = \{(0, 0), (1, \psi_1(r - 1)), (1, \psi_1(r + 1)), (2, f_0(1, r)), (2, f_1(1, r)), (2, f_2(1, r))\}.$$

Example 3.1 For the ring zone 1,

- $I_{1,0} = \{(0, 0), (1, 5), (1, 1), (2, 11), (2, 0), (2, 1)\}$
- $I_{1,5} = \{(0, 0), (1, 4), (1, 0), (2, 10), (2, 11), (2, 0)\}$.

The closest neighborhood of a virtual location (i, r) of the ring zone i, $1 < i < K - 1$, is

$$I_{i,r} = \{(i, \psi_i(r-1)), (i, \psi_i(r+1)), (i+1, f_0(i,r)), (i+1, f_1(i,r)), (i+1, f_2(i,r))\} \cup \{(i-1, r') \mid f_0(i-1, r') = r \text{ or } f_1(i-1, r') = r \text{ or } f_2(i-1, r') = r\}$$

Example 3.2 For the ring zone 2,

- $I_{2,1} = \{(2, 0), (2, 2), (3, 1), (3, 2), (3, 3), (1, 0), (1, 1)\}$
- $I_{2,2} = \{(2, 1), (2, 3), (3, 2), (3, 3), (3, 4), (1, 1)\}$
- $I_{2,3} = \{(2, 2), (2, 4), (3, 4), (3, 5), (3, 6), (1, 1), (1, 2)\}$.

The closest neighborhood of a virtual location in the outermost ring zone $K - 1$ is

$$I_{K-1,r} = \{(K-1, \psi_{K-1}(r-1)), (K-1, \psi_{K-1}(r+1))\} \cup \{(K-2, r') \mid f_0(K-2, r') = r \text{ or } f_1(K-2, r') = r \text{ or } f_2(K-2, r') = r\}$$

Example 3.3 For the outermost ring zone 9 in the case of $K = 10$,

- $I_{9,0} = \{(9, 55), (9, 1), (8, 49), (8, 0), (8, 1)\}$
- $I_{9,1} = \{(9, 0), (9, 2), (8, 0), (8, 1), (8, 2)\}$.

The notion of *closest neighborhood* is used in the following section to control the movement of fibers across virtual locations.

Yarn Model

Along a staple fiber yarn, new fibers arrive, migrate through virtual locations and then terminate. Given that a fiber has a smooth shape and does not break, the following definitions are useful for approximating a fiber path in the yarn structure presented in the previous section.

Definition 3.3

- At any yarn cross-section, a fiber is considered to be in the virtual location whose center is the closest to the fiber axis. When there are many such VLs, the fiber non-deterministically occupies one of them.
- A *migration distance* or *migration period* of a virtual location is defined to be the projection length of a fiber on the yarn axis from the position where the fiber enters that virtual location to the next position where the fiber leaves that virtual location (see Figure 4).
- The distance between the leading-ends of two fibers is defined to be the projection length on the yarn axis between the starting points of those fibers.

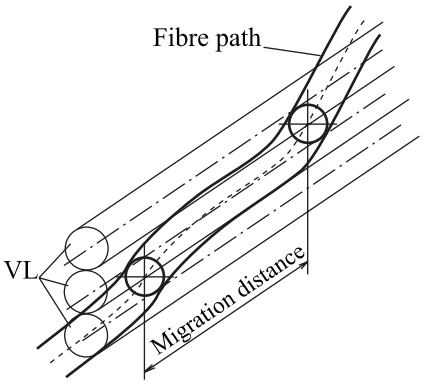

Figure 4 Migration distance.

The following assumptions are made on the yarn formation process:

1. The arrival of new fibers in a virtual location is a Poisson process. Therefore, the distances between the fiber leading-ends in a virtual location are exponentially distributed.
2. The migration distances (see Definition 3.3) are exponentially distributed.
3. The distances between the fiber leading-ends and the migration distances are mutually independent.
4. It is assumed that the process of yarn formation is continuous and hence there are infinitely many fibers involved in the process, i.e. the population size $E = \infty$.
5. Fibers are allocated into virtual locations on a FCFS basis.

Based on these assumptions, the structure of a staple fiber yarn can be modeled as a Jackson open network of $M/M/1$ queuing systems, where each queuing system models a virtual location. By analogy to the queuing theory presented in the previous sections, a fiber corresponds to a customer and a virtual location represents the server of the associated $M/M/1$ queuing system. At any time at most one fiber (customer) occupies a virtual location (server), although there might be many fibers waiting in the queue. The distances between fiber leading-ends correspond to the inter-arrival times of new customers and the migration distances correspond to the service times. From now on, the terms

time and *distance* (respectively, *customer* and *fiber*) are used interchangeably.

Suppose the distances between fiber leading-ends in a VL (i, r) are exponentially distributed with parameter λ_{ir}^0. Thus, a new fiber arrives to the VL (i, r) according to a Poisson process with rate λ_{ir}^0. After remaining in the VL (i, r) for a migration distance, which is exponentially distributed with parameter μ_{ir}, the fiber either terminates with probability p_{ir}^0 or migrates into a VL (j, s) with probability $p_{ir;js}$. It is assumed that a fiber can only take an elementary migration action (see Definition 3.2) in any single migration step. Therefore, the probability $p_{ir;js}$ for a fiber to migrate in one step from the VL (i, r) to the VL (j, s) is 0 if the VL (j, s) is not in the closest neighborhood I_{ir} of the VL (i, r). Let E_i denote the set of all VLs in the ring zone i; $E_0 = \{0\}$ and $E_i = \{x \in N | 0 \le x < \lfloor 2\pi i \rfloor\}$, for $i > 0$. The normalization condition in equation (3) must be re-written as follows:

$$\left(\sum_{(j,s) \in I_{ir}} p_{ir;js} \right) + p_{ir}^0 = 1,$$

$$\text{for } 0 \le i < K \text{ and } 0 \le r < |E_i|. \tag{7}$$

In the same way, equation (5) takes the form as follows:

$$\lambda_{ir} = \lambda_{ir}^0 + \sum_{j=0}^{K-1} \sum_{s=0}^{|E_j|-1} p_{js;ir} \lambda_{js},$$

$$\text{for } 0 \le i < K \text{ and } 0 \le r < |E_i|. \tag{8}$$

The system state is characterized by a vector $(n_{00}, n_{10}, \ldots, n_{K-1, \lfloor 2\pi(K-1) \rfloor - 1})$, such that each component n_{ir} is the number of fibers in the queuing system modeling the VL (i, r), $0 \le i < K$ and $0 \le r < |E_i|$. The steady-state probability of the network of queues modeling the yarn being in a given state is given by the probability density function δ defined in equation (4). In the following sections, this probability is used to analyze the structural properties of the yarn.

Deriving the Distribution of the Number of Fibers in Ring Zones from the Steady-state Probability

Because in a Jackson open network of queuing systems at steady-state each queuing system behaves as if it were independent, the marginal probability $\delta_{ir}(n)$ of the number of fibers in the queuing system associated to the VL (i, r) being exactly n is given by equation (1), viz.

$$\delta_{ir} = \tau_{ir}(n).$$

In the queuing model of a staple fiber yarn presented in the previous section, each VL represents the server of the $M/M/1$ queuing system associated to that VL. It follows that a VL is empty if the associated queuing system is empty and is occupied if that queuing system is not empty. Therefore, if 0 denotes the state of an empty VL and 1 that of an occupied VL, the probability of a VL (i, r) being in state $b \in \{0, 1\}$, $\tau_{ir}^*(b)$, is defined as follows:

$$\tau_{ir}^*(0) = \tau_{ir}(0) = 1 - \rho_{ir}, \quad \tau_{ir}^*(1) = 1 - \tau_{ir}(0) = \rho_{ir}. \tag{9}$$

Thus, the occupancy probability of a VL (i, r) is equal to the traffic intensity $\rho_{ir} = \lambda_{ir}/\mu_{ir}$ of the associated $M/M/1$ queuing system.

The state of a yarn cross-section is characterized by a vector $(b_{00}, b_{10}, \ldots, b_{K-1, \lfloor 2\pi(K-1) \rfloor - 1})$, such that each component b_{ir} is the state of the VL (i, r), where $0 \le i < K$ and $0 \le r < |E_i|$. The steady-state probability of a yarn cross-section being in a given state, δ^*, is defined by

$$\delta^*(b_{00}, b_{10}, \ldots, b_{K-1, \lfloor 2\pi(K-1) \rfloor - 1}) = \prod_{i=0}^{K-1} \prod_{r=0}^{|E_i|-1} \tau_{ir}^*(b_{ir}). \tag{10}$$

Let $S_n(X)$ denote the set of all subsets of the set X having exactly n elements. Let $X \backslash Y$ denote the set difference of X and Y, i.e. the set of all elements of the set X which are not elements of the set Y. The distribution of the number of fibers in ring zones is then defined by:

$$\sigma_i(n) = \sum_{X \in S_n(E_i)} \left(\prod_{r \in X} \tau_{ir}^*(1) \prod_{s \in (E_i \backslash X)} \tau_{is}^*(0) \right),$$

$$\text{for } 0 \le i < K \text{ and } 0 \le r < |E_i| \tag{11}$$

Because the set E_i has $2^{|E_i|}$ possible subsets, the computational complexity of σ_i in equation (11) is $O\left(2^{|E_i|}\right)$, where $|E_i|$ is the number of virtual locations in the zone i. Therefore, in general it is computationally difficult to calculate σ_i for a high value of i. However, in the case where the occupancy probability is the same for all the VLs of the same zone, equation (11) simplifies to a binomial distribution as follows:

$$\sigma_i(n) = \binom{|E_i|}{n} \left(\tau_i^*\right)^n \left(1 - \tau_i^*\right)^{|E_i| - n},$$

$$\text{for } 0 \le i < K \text{ and } 0 \le n < |E_i| \tag{12}$$

where $\binom{|E_i|}{n}$ is the number of subsets of the set E_i that have exactly n elements; τ_i^* is the occupancy probability of the ring zone i and is defined by $\tau_i^* = \frac{1}{|E_i|}\sum_{r=0}^{|E_i|-1}\tau_{ir}^*(1)$.

$\sigma_i(n)$ is the probability of the number of fibers in the ring zone i being n, for $0 \le i < K$ and $0 \le n \le |E_i|$.

Using this, the following characteristics of a yarn structure can be calculated:

Average Number of Fibers in Ring Zones
The average number of fibers in a ring zone i is

$$\overline{N}_i = \sum_{n=1}^{|E_i|} n\sigma_i(n), \quad \text{for } 0 \le i < K \tag{13}$$

Average Number of Fibers in a Yarn Cross-section
The average number of fibers in a yarn cross-section is

$$\overline{N} = \sum_{i=0}^{K-1} \overline{N}_i \tag{14}$$

Average Yarn Linear Density
Given the average linear density of the fibers, $\overline{D}_f$, the average linear density of the yarn is

$$\overline{N} \times \overline{D}_f$$

Average Yarn Packing Fraction
The average yarn packing fraction, $\bar{\phi}$, can be defined as follows:

$$\bar{\phi} = \frac{\text{area of the yarn cross-section occupied by fibers}}{\text{area of the yarn cross-section}}$$

$$= \frac{\pi(\bar{d}_f/2)^2\overline{N}}{\pi((2K-1)((\bar{d}_f+\sigma_f)/2))^2}$$

$$= \frac{\overline{N}}{(2K-1)^2(1+c_d)^2},$$

where $\bar{d}_f$ and σ_f are the average and the standard deviation of the fibers' diameters, respectively; $c_d = \sigma_f/\bar{d}_f$ is the variation coefficient of fiber diameter.

For example:

- $K = 0$ implies that there are no fibers, $\overline{N} = 0$, and thus

$$\bar{\phi} = \frac{\overline{N}}{(2K-1)^2(1+c_d)^2} = \frac{0}{(-1)^2(1+c_d)^2} = 0;$$

- $K = 1$ implies that there is a single fiber in the yarn, $\overline{N} = 1$, in which case

$$\bar{\phi} = \frac{\overline{N}}{(2K-1)^2(1+c_d)^2} = \frac{1}{(1)^2(1+c_d)^2} = \frac{1}{(1+c_d)^2};$$

- $K = 2$ implies that $1 \le \overline{N} \le 7$ which yields $\frac{1}{9(1+c_d)^2} \le \bar{\phi} \le \frac{7}{9(1+c_d)^2}$.

If we assume that the variation in fiber diameter is small, then the formula for the average packing fraction can be simplified to give

$$\bar{\phi} = \frac{\overline{N}}{(2K-1)^2}.$$

Degree of Migration

The probability p_{ij} of a fiber to migrate from a ring zone i to a ring zone j is obtained from the probability distribution of fiber migration between virtual locations, $p_{ir;js}$, presented in the Yarn Model section by taking the normalized sum of the probabilities for migrating from a VL in the ring zone i to a VL in the ring zone j, viz.

$$\left.\begin{aligned} p_{01} &= \sum_{r=0}^{5} p_{00;1r}, \text{ if } i = 0; \\ p_{ij} &= \frac{1}{\lfloor 2\pi i \rfloor}\sum_{r=0}^{\lfloor 2\pi i \rfloor - 1}\sum_{(j,s)\in I_{ir}} p_{ir;js}, \text{ if } i > 0; \end{aligned}\right\} \tag{15}$$

where I_{ir} is the closest neighborhood of the VL (i, r). Therefore, $p_{ij} = 0$ when $|j - i| > 1$ as an elementary migration can only happen within a ring zone or between two adjacent ring zones (see Definition 3.2).

Similarly, the probability p_i^0 of a fiber terminating in a ring zone i is

$$\left.\begin{aligned} p_0^0 &= p_{00}^0, \text{ if } i = 0; \\ p_i^0 &= \frac{1}{\lfloor 2\pi i \rfloor}\sum_{r=0}^{\lfloor 2\pi i \rfloor - 1} p_{ir}^0, \text{ if } i > 0 \end{aligned}\right\} \tag{16}$$

Given the fiber migration distributions between ring zones, it is possible to calculate the average number of fibers that migrate inwards, outwards or stay in each ring zone.

It has been shown in equation (13) that the average number of fibers $\overline{N}_i$ in a ring zone i can be calculated from the yarn model. Thus, the average number of fibers in zone i that

- migrate inwards is $p_{i,i-1}\overline{N}_i$ if $i > 0$ and 0 if $i = 0$,
- migrate outwards is $p_{i,i+1}\overline{N}_i$ if $i < K-1$ and 0 if $i = K-1$,
- remain in the zone is $p_{ii}\overline{N}_i$,

for $0 \le i < K$.

The notion of degree of migration defined in Definition 3.4 is an estimate of the degree of fiber entanglement in a yarn. It should be noted that the angular positions of fibers in the ring zones are directly affected by the yarn twist level, which is an important characteristic of the yarn structure. It should be expected that the probability for a fiber to migrate from a given VL in the direction coinciding with the twist direction would be greater than that for the migration against the twist. In the case of a melange yarn, changes in angular position of fibers have incidences on the color properties of the mixture.

Definition 3.4

- The *degree of inwards migration* of a staple fiber yarn is defined to be the proportion of fibers in each cross-section of the yarn that migrate inwards and is denoted by

$$D_{in} = \frac{\sum_{i=1}^{K-1} p_{i,i-1}\overline{N}_i}{\sum_{i=0}^{K-1} \overline{N}_i}.$$

- Similarly, the *degree of outwards migration* of a staple fiber yarn is defined to be the proportion of fibers in each cross-section of the yarn that migrate outwards and is denoted by

$$D_{out} = \frac{\sum_{i=0}^{K-2} p_{i,i+1}\overline{N}_i}{\sum_{i=0}^{K-1} \overline{N}_i}.$$

- The *degree of migration* of a staple fiber yarn is defined to be the proportion of fibers in each cross-section of the yarn that migrate inwards or outwards and is denoted by

$$D = D_{in} + D_{out}.$$

The degree of migration affects the color of the melange yarn; this is particularly true for the outer zones of the yarn. The degree of migration defines the frequency with which fibers of different color appear on and close to the yarn surface where fibers are most visible and are not masked by the fibers above. The degree of migration also defines the uniformity of color blend; higher migration means that fibers of different color may have better chances to mix. A higher degree of migration leads to a shorter visible length of fiber of every color in the blend. Thus, over the unit length of the yarn colors are mixed by smaller units making the color appearance more uniform.

Estimation of the Number of Contact Points Between Fibers Due to Migration

The process of fiber migration creates points of contact between fibers. The friction between fibers at the contact points increases the strength of the yarn and its ability of self-locking when stretched. Early studies [20] have shown that the minimum possible number of fibers in a worsted spun staple yarn cross-section should be between 30 and 40, otherwise the friction between the fibers will be insufficient to hold them together. If all other yarn characteristics are fixed, then the greater degree of migration should lead to the greater number of contact points between fibers in a yarn, which in turn should mean a stronger yarn. The degree of migration and the number of contact points cannot be infinitely large; they are both limited by the fiber dimensions. This has been discussed by Pan [21] and Komori and Itoh [22] in their studies of general fiber assemblies. Moreover, a greater degree of migration leads to the fibers being oriented off the direction parallel to the yarn axis; this decreases their contribution to the total strength of the yarn. Thus, the maximum strength of the yarn may be achieved not at the point of the maximum possible number of contact points but at the number that is sufficient to provide necessary cohesion between the fibers.

This section presents an approach for computing the average number of contact points between fibers that may occur within a migration distance. Recall that a migration event takes place if a fiber changes its virtual location. A contact point between fibers may occur due to the fibers having natural crimp. However, the approach does not take into account situations where two fibers touch each other without changing their virtual location as depicted in Figure 5. It is also assumed that linear contacts between fibers do not occur due to the physical properties of fibers.

There are 13 different cases when fiber migration may lead to the fibers making contact points; they are presented in Figure 6 where the twist direction, T, is assumed to be clockwise. Each of these cases represents a fiber migration pattern that generates contact points between the fibers

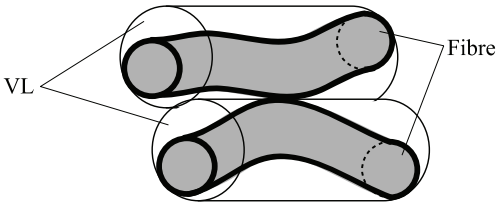

Figure 5 Example of a contact point between fibers without migration

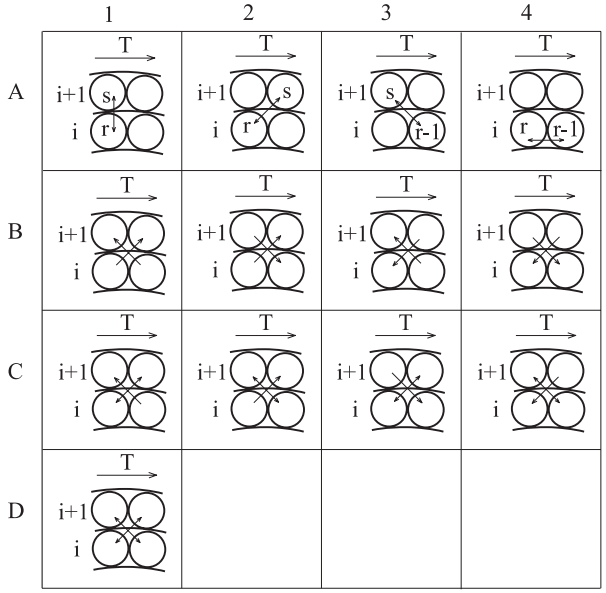

Figure 6 Fiber migration patterns that generate points of contact.

involved. The three neighborhood functions f_0, f_1 and f_2 defined in equation (6) are useful to understand the occurrence of the fiber migration patterns.

In Figure 6, each of the four fiber migration patterns in the row A occurs when two fibers occupying two neighboring VLs migrate by exchanging their positions. An occurrence of such a pattern generates exactly one contact point between the two migrating fibers. A fiber migration pattern $A1$ occurs when a fiber in a VL (i, r) and a fiber in the VL $(i + 1, f_1(i, r))$ exchange their positions. Similarly, a fiber migration pattern $A2$ occurs when a fiber in a VL (i, r) and a fiber in the VL $(i + 1, f_0(i, r))$ exchange their positions. In the same way, a fiber migration pattern $A3$ occurs when a fiber in a VL (i, r) and a fiber in the VL $(i + 1, f_2(i, r))$ exchange their positions. Unlike the first three patterns which require fibers to change their ring zones (i.e. radial migration), the fiber migration pattern $A4$ requires fibers occupying two neighboring VLs of the same ring zone to migrate by exchanging their positions (i.e. angular migration).

Table 2 Maximum number of occurrences of a pattern in a ring zone having m virtual locations.

	1	2	3	4
A	m	m	m	$\lfloor m/2 \rfloor$
B	$\lfloor m/2 \rfloor$	$\lfloor m/2 \rfloor$	$\lfloor m/2 \rfloor$	$\lfloor m/2 \rfloor$
C	$\lfloor m/2 \rfloor$	$\lfloor m/2 \rfloor$	$\lfloor m/2 \rfloor$	$\lfloor m/2 \rfloor$
D	$\lfloor m/2 \rfloor$			

The fiber migration pattern $B1$ occurs when the fiber in a virtual location $(i, \psi_i(2n-1))$ of a ring zone i migrates outwards into the virtual location $(i+1, f_2(i, \psi_i(2n-1)))$ of the ring zone $i+1$, while another fiber migrates outwards from the virtual location $(i, 2n)$ of the ring zone i into a virtual location $(i+1, f_0(i, 2n))$ of the ring zone $i+1$, for some n such that $0 \le n < \lfloor \lfloor 2\pi i \rfloor / 2 \rfloor$. This generates exactly one contact point between the two fibers involved. The patterns $B2$, $B3$ and $B4$ occur in a similar manner.

The migration patterns $C1$ to $C4$ involve three fibers in two adjacent ring zones of which two exchange their positions and the third fiber migrates into a non-occupied or vacated VL; each of these patterns may generate three contact points between the fibers involved.

The migration pattern $D1$ presents a specific case involving two pairs of fibers where fibers of each pair exchange their positions between two neighboring ring zones. The occurrence of this pattern may lead to the formation of six contact points between the fibers.

It is interesting to be able to estimate the average number of contact points in a yarn cross-section that are generated by these patterns. A pattern of type A or B generates exactly one contact point, while a type C pattern generates three contact points and a type D pattern generates six contact points. It is reasonable to assume that the number of contact points in a cross-section generated by occurrences of a given migration pattern is proportional to the number of occurrences of that pattern. The maximum number of occurrences of each migration pattern in a ring zone i of a yarn cross-section is given in Table 2, where m is the number of VLs in the ring zone i, $0 \le i < K$. This is depicted in Figures 7 and 8 for ring zone 2. Note that the only migration pattern that can occur between the VLs in the outermost ring zone is $A4$, while the migration pattern $A1$ is the only one that can occur between ring zone 0 and ring zone 1.

More importantly, the probability distribution of the number of occurrences of each migration pattern can be calculated using the occupancy probabilities of VLs and the probabilities of a fiber to migrate from one VL to another

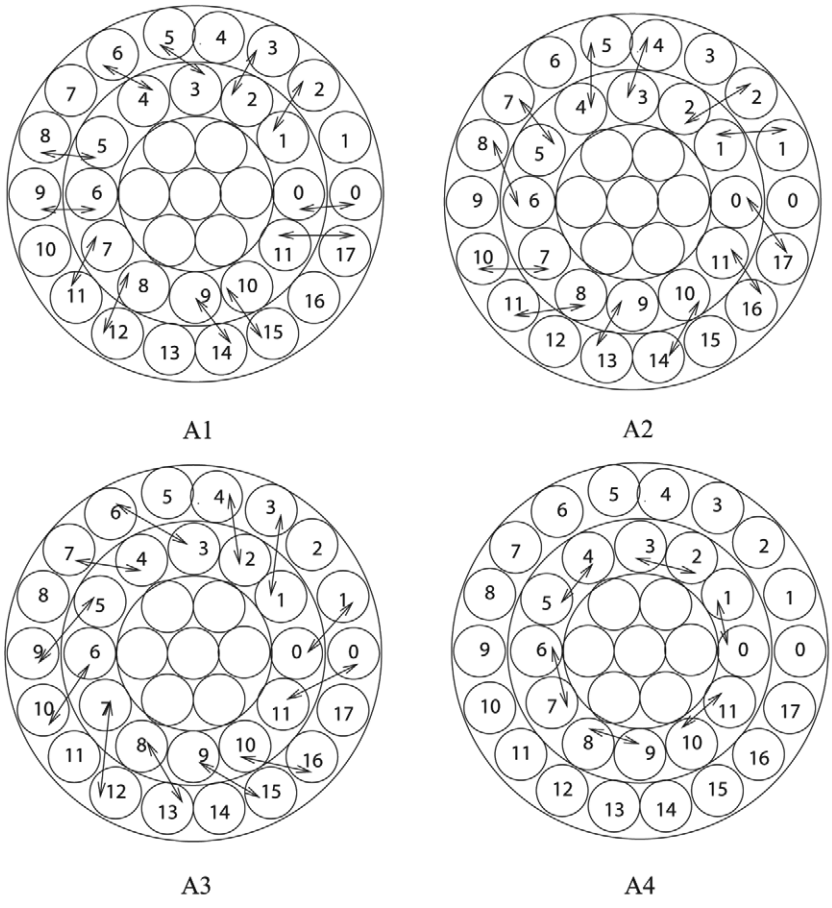

Figure 7 Two fibers in two neighbouring zones exchange their positions.

VL. For example, the probability of a pattern $A4$ to occur between two neighboring VLs $(i, \psi_i(r-1))$ and (i, r), denoted by $A4(i, r)$, is equal to the probability that the two virtual locations are occupied and each fiber migrates into the other's virtual location, i.e.

$$A4(i,r) = \rho_{ir} \times p_{ir;\, i\,\psi(r-1)} \times \rho_{i\,\psi(r-1)} \times p_{i\,\psi(r-1);\, ir}, \qquad (17)$$

where ρ_{xy} is the occupancy probability of the virtual location (x, y) defined in equation (9); $p_{xt;\, yu}$ is the probability for a fiber to migrate from the VL (x, t) to the VL (y, u).

Let $\theta_i(n)$ denote the probability of the number of patterns $A4$ occurring in the ring zone i being n. It follows that

$$\theta_i(n) = \sum_{X \in S_n(F_i)} \left(\prod_{r \in X} A4(i,r) \times \prod_{s \in (F_i \setminus X)} (1 - A4(i,s)) \right),$$

$$\text{for } 0 \le i < K \qquad (18)$$

where $F_i = \{2x \mid x \in N \text{ and } 0 \le x < \lfloor \lfloor 2\pi i \rfloor / 2 \rfloor\}$.

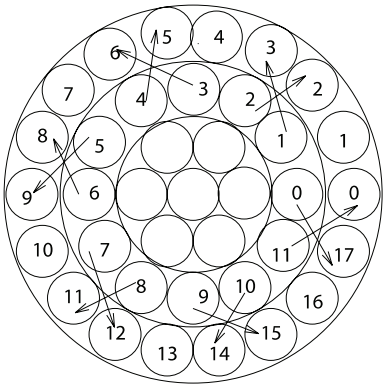

Figure 8 An example of B1 migration pattern.

The computational complexity of $\theta_i(n)$ as defined in equation (18) is $O\left(2^{|F_i|}\right)$. Hence, it is costly to compute θ_i for high values of i in general. However, if $A4(i, r) = A4(i, s)$ for any pair $(r, s) \in F_i$ then equation (18) reduces to

Table 3 Migration patterns' probabilities.

$A1(i, r) = \rho_{ir} \times p_{ir;\,(i+1)\,f_1(i,r)} \times \rho_{(i+1)\,f_1(i,r)} \times p_{(i+1)\,f_1(i,r);\,ir}$

$A2(i, r) = NE(i, r) \times SW(i, r) \times (1 - NW(i, \psi_i(r-1))) \times (1 - SE(i, \psi_i(r-1)))$

$A3(i, r) = NW(i, \psi_i(r-1)) \times SE(i, \psi_i(r-1)) \times (1 - NE(i, r)) \times (1 - SW(i, r))$

$B1(i, r) = NE(i, r) \times NW(i, \psi_i(r-1)) \times (1 - SE(i, \psi_i(r-1))) \times (1 - SW(i, r))$

$B2(i, r) = NE(i, r) \times SE(i, \psi_i(r-1)) \times (1 - SW(i, r)) \times (1 - NW(i, \psi_i(r-1)))$

$B3(i, r) = NW(i, \psi_i(r-1)) \times SW(i, r) \times (1 - NE(i, r)) \times (1 - SE(i, \psi_i(r-1)))$

$B4(i, r) = SE(i, \psi_i(r-1)) \times SW(i, r) \times (1 - NE(i, r)) \times (1 - NW(i, \psi_i(r-1)))$

$C1(i, r) = SW(i, r) \times NE(i, r) \times NW(i, \psi_i(r-1)) \times (1 - SE(i, \psi_i(r-1)))$

$C2(i, r) = NW(i, \psi_i(r-1)) \times SE(i, \psi_i(r-1)) \times NE(i, r) \times (1 - SW(i, r))$

$C3(i, r) = SW(i, r) \times NE(i, r) \times SE(i, \psi_i(r-1)) \times (1 - NW(i, \psi_i(r-1)))$

$C4(i, r) = NW(i, \psi_i(r-1)) \times SE(i, \psi_i(r-1)) \times SW(i, r) \times (1 - NE(i, r))$

$D1(i, r) = SW(i, r) \times NE(i, r) \times NW(i, \psi_i(r-1)) \times SE(i, \psi_i(r-1))$

$$\theta_i(n) = \binom{|F_i|}{n} (A4(i,0))^n (1 - A4(i,0))^{(|F_i| - n)},$$

$$\text{for } 0 \le i < K. \tag{19}$$

Equation (19) is easier to calculate than equation (18) because there is no need to construct the set $S_n(F_i)$.

Given the probability distribution $\theta_i(n)$ of the number of the occurrences of the migration pattern $A4$ in a ring zone i of a yarn cross-section, the average number $\overline{M}_i$ of occurrences of the migration pattern $A4$ is calculated as follows:

$$\overline{M}_i = \sum_{n=1}^{|F_i|} n\theta_i(n). \tag{20}$$

The probability distribution of the number of occurrences for each of the other migration patterns is defined as in equation (18), where $A4$ is replaced by the corresponding function in Table 3, where

- $NE(i, r) = \rho_{ir} \times p_{ir;\,(i+1)f_0(i,r)}$ is the probability of the VL (i, r) being occupied and a fiber migrates outwards from the VL (i, r) to the VL $(i + 1, f_0(i, r))$
- $SW(i, r) = \rho_{(i+1),f_0(i,r)} \times p_{(i+1)f_0(i,r);\,ir}$ is the probability of the VL $(i + 1, f_0(i, r))$ being occupied and a fiber migrates inwards from the VL $(i + 1, f_0(i, r))$ to the VL (i, r)
- $NW(i, r) = \rho_{ir} \times p_{ir;\,(i+1)f_2(i,r)}$ is the probability of the VL (i, r) being occupied and a fiber migrates outwards from the VL (i, r) to the VL $(i + 1, f_2(i, r))$
- $SE(i, r) = \rho_{(i+1),f_2(i,r)} \times p_{(i+1)f_2(i,r);\,ir}$ is the probability of the VL $(i + 1, f_0(i, r))$ being occupied and a fiber migrates inwards from the VL $(i + 1, f_2(i, r))$ to the VL (i, r)

The average number of contact points created in a ring zone i by occurrences of a given migration pattern is proportional to the average number of occurrences of that migration pattern and is equal to

$$\gamma \times \overline{M}_i \tag{21}$$

where γ is the number of contact points created by a single occurrence of that migration pattern. The value of γ is 1 for type A patterns and type B patterns, 3 for type C patterns and 6 for type D patterns, see Figure 6.

The analysis of equation (18) and Table 3 shows that the probabilities of fibers to create different patterns are different and depend on the number of fibers involved and the direction of migration relative to the twist direction. It can be assumed that the likelihood of a fiber migrating against the twist direction is much lower than that coinciding with the twist direction. It is also obvious that the cases involving two fibers are more likely to occur than those involving three or four fibers.

Experiments

In order to validate the yarn model presented above, two experiments were conducted. The first experiment aimed at determining the effects of yarn linear density and twist factor of melange yarns on the distribution of the number of fibers in the ring zones by analyzing yarn cross-sections. The objective of the second experiment was to study the effects of the same parameters on fiber migration patterns using the *tracer-fiber* technique, first described by Morton and Yen [23] and later widely used in the literature [1, 15]. Both experiments were carried out on four samples of ring-spun staple fiber yarn that differed in linear density and/or twist factor. All samples were conditioned and tested at standard temperature of 20 ± 2 °C and relative humidity of 65 ± 2 % according to BS EN 20139:1992 [24]. The fiber used for the production of melange yarns was Polyacrylic. The average fiber length was estimated using WIRA Fiber Diagram Machine; the average fiber diameter was estimated by measuring 5, 000 fiber snippets using LaserScan tester, see Table 4.

The specifications of the yarn samples are given in Table 5, where samples $S1$, $S2$ and $S4$ were of the same linear density but different twist factor; samples $S3$ and $S4$ had almost the same twist factor but different linear densities. The twist factor, α, was calculated using the formula according to BS EN 2061:1996 [25] as follows:

$$\alpha = t\sqrt{\frac{\bar{T}_y}{1000}},$$

Table 4 Fiber properties.

Fiber type	Average fiber length, mm	Standard deviation of fiber length, mm	Average fiber diameter, μm	Standard deviation of fiber diameter, μm
Red	98.8	38.5	23.2	3.6
Green	95.3	38.8	23.5	3.0
Blue	97.7	37.3	23.8	3.1
White	103.9	39.6	24.5	3.7
Black	97.4	37.2	24.4	3.4

Table 5 Specifications of yarn samples.

Sample	Linear density, tex	Twist level, tpm	Twist factor, a
*S*1	55	674	158.1
*S*2	55	337	79.0
*S*3	90	395	118.5
*S*4	55	505	118.4

where t is the yarn twist, in turns per meter; $\overline{T}_y$ is the yarn linear density, expressed in tex.

The original tow was converted to staple sliver by stretch breaking on a Seydel Converter. In the first experiment, slivers of red, green and blue polyacrylic fiber were processed to a melange yarn using a traditional Platt reduction line. This included three passages of gilling for intimate blending of equal proportions of slivers with auto leveling at the last passage followed by roving and ring spinning. Thirty independent 0.5 m-long yarn specimens were randomly taken at least 2 m apart from each of four yarn samples. The middle part of each specimen was then embedded into Technovit 7100® resin in an 8 mm diameter gelatine capsule and a cross-section was taken from each of the melange yarn specimens using an MR2/S200 Boeckeler microtome. The images of these cross-sections, captured with an Olympus SZX9 microscope fitted with an Olympus C-7070 digital camera, were processed using software specially developed for this purpose. The software identifies the radial and the angular positions of individual fibers of each color in the yarn cross-section relative to the yarn center, which is approximated by the center of gravity of the cross-section. The software then calculates the ring zone and the virtual location occupied by fiber of each color in the cross-section under the assumption that a fiber occupies the virtual location that is the closest to the fiber center (see Definition 3.3). Using these data, the distribution of the average number of fibers of all three colors together in ring zones has been estimated; examples of this distribution are depicted in Figure 9(a). The analysis of the distribution of each individual color will be presented in

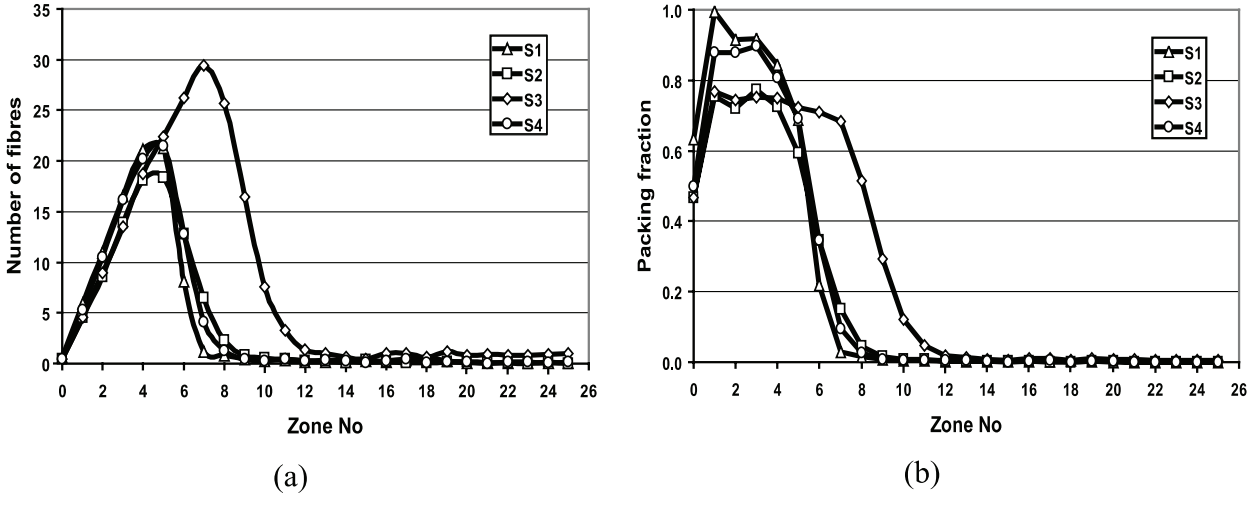

Figure 9 Experimental distribution of the average number of fibres (a) and fiber packing density (b) in ring zones.

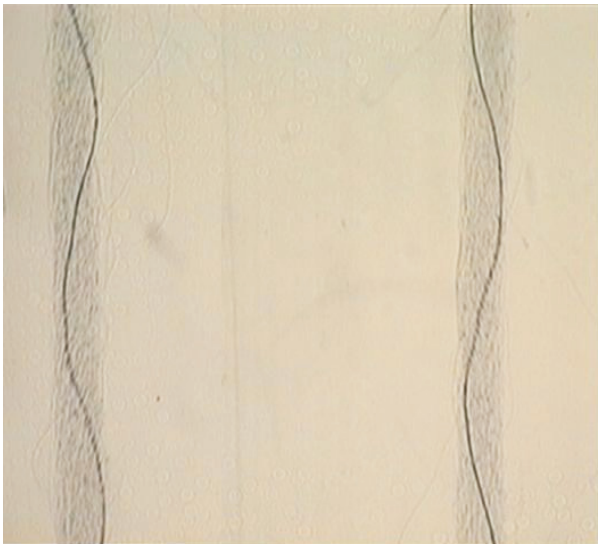

Figure 10 An example of a tracer fiber image

Part III of the paper. Fiber packing density in the yarn cross-section has been characterized by fiber packing fraction in each ring zone i, ϕ_i, which was estimated as the ratio of the number of fibers in the ring zone, $\overline{N}_i$, to the number of virtual locations in the zone, $|E_i|$:

$$\phi_i = \frac{\overline{N}_i}{|E_i|} \quad ,$$

where E_i is the set of all VLs in the ring zone i, $1 \le i \le K-1$ and K is the number of ring zones.

The experimental distribution of fiber packing density in ring zones is presented in Figure 9(b).

The second experiment applied the *tracer-fiber* technique to yarn samples of the same linear density and twist factor as in the first experiment (see Table 5). Yarns were ring spun using white polyacrylic fibers mixed with 0.5 % of black fibers added to serve as tracer fibers. Data on fiber length and diameter are presented in Table 4. From every yarn sample, 15 portions of the yarn containing an individual tracer fiber were randomly selected for analysis. Figure 10 shows two images of a tracer-fiber in a yarn body taken simultaneously from two perpendicular directions using a front-surface mirror positioned at a 45° angle to the camera. The two images were used to calculate the 3D path of the tracer-fiber in the yarn. Image processing software was specially developed to extract migration information from these images, which on average provided some 900 fiber migrations between virtual locations for every yarn portion. This enabled very detailed information on yarn structure to be obtained, which included such characteristics as the probabilities of fibers to migrate between virtual locations (see Figure 11), the average migration distance of virtual locations and spatial position of individual fibers with respect to the yarn axis (Figure 12(a) and (b)).

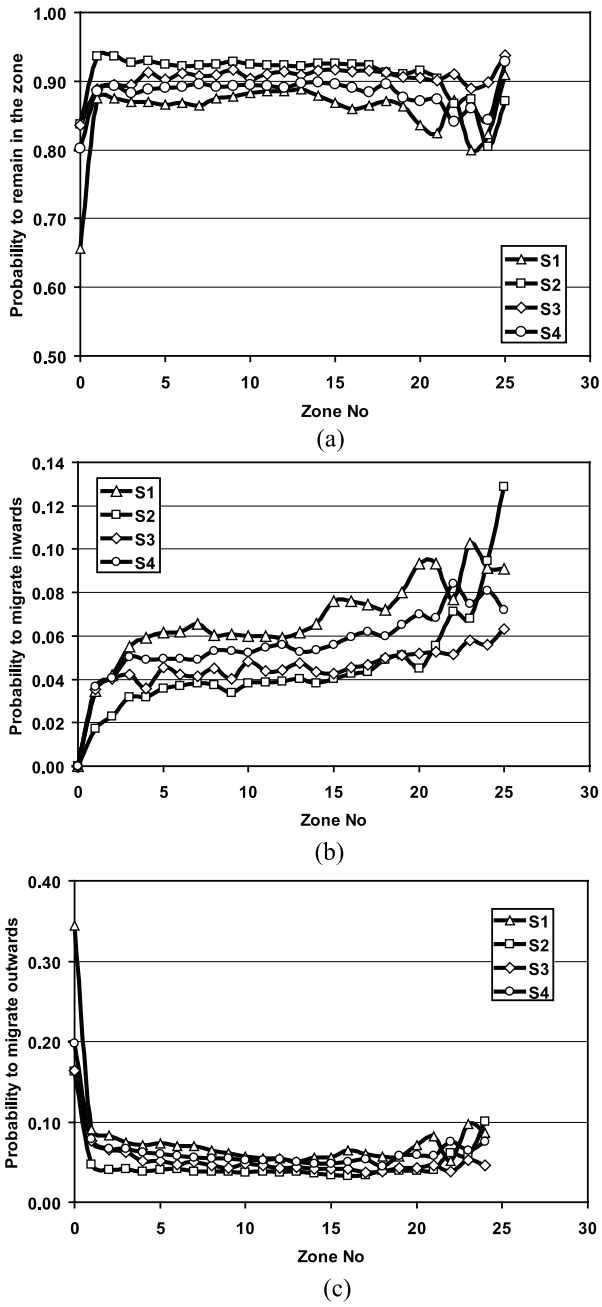

Figure 11 Migration probabilities: (a) to remain in the zone; (b) to migrate inwards; (c) to migrate outwards.

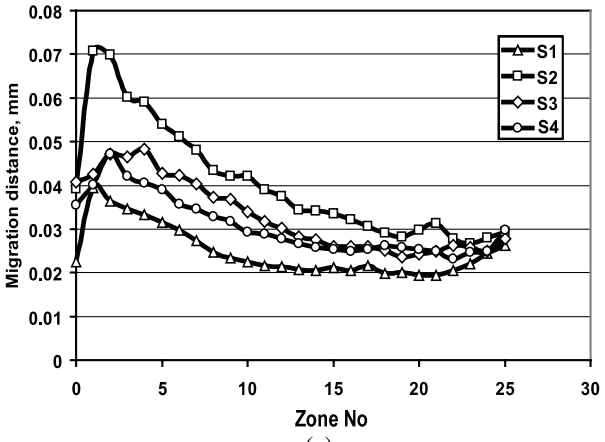

(a)

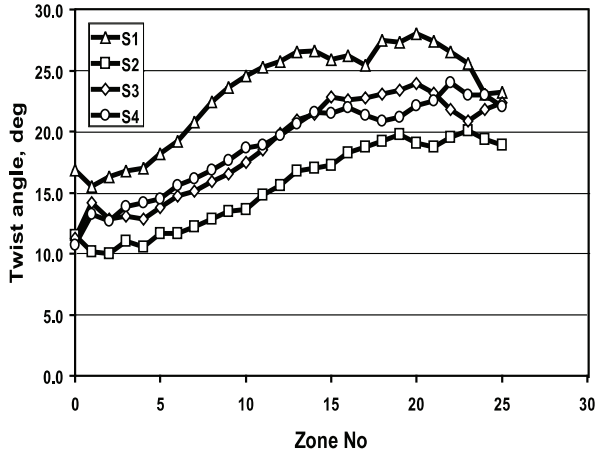

(b)

Figure 12 Migration distance (a) and yarn twist angle (b).

It has been shown in the Computing the Closest Neighbors of a VL section that, using symmetry in the neighborhood relationship, the migration probabilities can be further split into three components which define the direction of migration relative to the direction of yarn twist. Let p_+ and p_- be the probabilities for a fiber to migrate outwards from its original virtual location into the virtual location which is the next in the direction of twist and in the direction opposite the twist, respectively; these virtual locations are defined by functions f_0 and f_2 in equation (6), respectively. Let p_0 be the probability for the fiber to migrate outwards into the VL defined by function f_1, equation (6). In a similar way, the probability to remain in a zone or to migrate inwards can be split according to the twist direction into p_+, p_0 and p_-. As an example, probabilities p_+, p_0 and p_- for sample $S4$ are presented in Figure 13(a), (b), and (c), respectively.

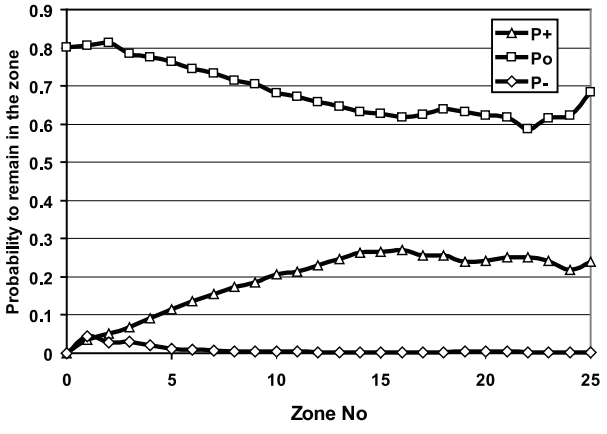

(a)

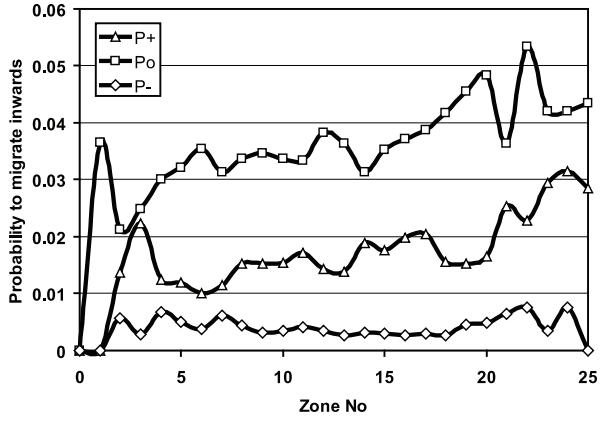

(b)

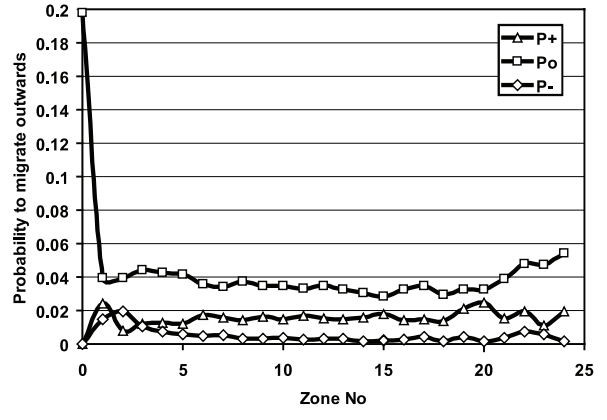

(c)

Figure 13 Migration probabilities for sample S4: (a) to remain in the zone; (b) to migrate inwards; (c) to migrate outwards.

The migration probabilities were substituted in the system of linear equations equation (8) and this system was solved in MatLab® to determine the arrival rates of fibers in virtual locations, λ_{ir}. The total arrival rate of new fibers, λ^0, was estimated through the total average number of fibers in the yarn cross-section, $\overline{N}$, and the average fiber length, $\overline{L}_f$, using Little's law [17]:

$$\lambda^0 = \overline{N}/\overline{L}_f.$$

The arrival rate of new fibers to each individual VL was estimated as

$$\lambda_{ir}^0 = \frac{R_i \lambda^0}{|E_i|},$$

where $R_i = \frac{\rho_i}{\sum_{j=0}^{K-1} \rho_j}$; $\rho_i = \frac{\overline{N}_i}{|E_i|}$; $\overline{N}_i$ is the average number of fibers in the zone i and E_i is the set of all VLs in the ring zone i.

Knowing the arrival rate and the average migration distance (i.e. the average service time in Queuing Theory terminology) of each virtual location, the occupancy probability of each virtual location was calculated as in equation (9). Then the distribution of the number of fibers in ring zones was predicted by the model using equation (11); an example of such distribution for sample *S*1 is presented in Figure 14. This distribution was used to predict the distribution of the average number of fibers in ring zones (see equation (13) and Figure 15(a)) and the distribution of fiber packing density (Figure 15(b)).

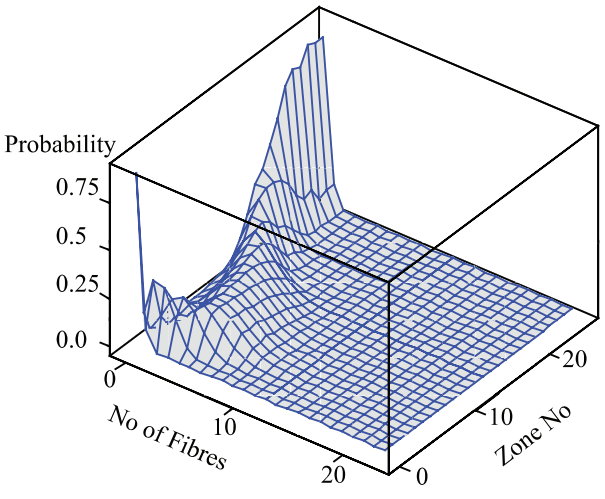

Figure 14 Predicted distribution of the number of fibers in ring zones for sample S1.

Discussion

The analysis of the yarn cross-sections showed that the number of fibers in a ring zone is a random variable that follows an unknown distribution. It appears that ring zones are more populated towards the yarn center, leading to a compact body covered by loosely entangled fibers which degenerate into hairiness.

The comparison of the distributions of fiber packing fraction in ring zones between the samples (see Figure 9(b)) showed a similar change in the shape of the distributions to earlier published results [26, 27]. In particular, it can be seen from Figure 9(b) that increasing yarn linear density leads to more widespread distributions with nearly constant density of fibers over a significant part of yarn body (samples *S*4 and *S*3), whereas increase in twist factor makes the yarn more compact with fibers concentrating in central zones (samples *S*2, *S*4 and *S*1).

Experimentally estimated migration probabilities of fibers in Figure 11 showed the same general relationship against fiber radial position as that reported earlier [15].

The analysis of the migration probabilities (Figure 13) showed that for all samples studied the probability p_0 was much higher than the probability to migrate in the direction of twist, p_+, which in turn was higher than the probability to migrate against the twist direction, p_-.

The migration probability distributions for samples *S*1, *S*2 and *S*3 have been compared with those for sample *S*4 using Pearson's χ^2 criterion; the results are presented in Table 6. The calculated values of the criterion were far greater than the critical value of 36.415 at $df = 24$ and significance level of 0.05, and even greater than the critical value of 42.980 at $df = 24$ and significance level of 0.01. Thus, it can be assumed that within the range of yarn parameters studied both linear density and twist factor have an effect on migration probabilities. A more detailed investigation is required to understand the degree of this effect.

The migration distance was found to be in an inverse proportion to the twist factor (Figure 12(a) and (b)). This was in agreement with the relationship between the twist factor and the probability to remain in the zone. Indeed, let us consider probabilities in Figure 11(a), (b) and (c) together with migration distance and twist angle in Figure 12(a) and (b) for yarn samples of the same linear density in the order of increasing twist factor, i.e. samples *S*2,

Table 6 Values of χ^2 criterion.

Sample	Migration within the zone	Inwards migration	Outwards migration
S1	336.1	253.1	265.0
S2	193.1	45.6	48.6
S3	185.0	93.7	90.3

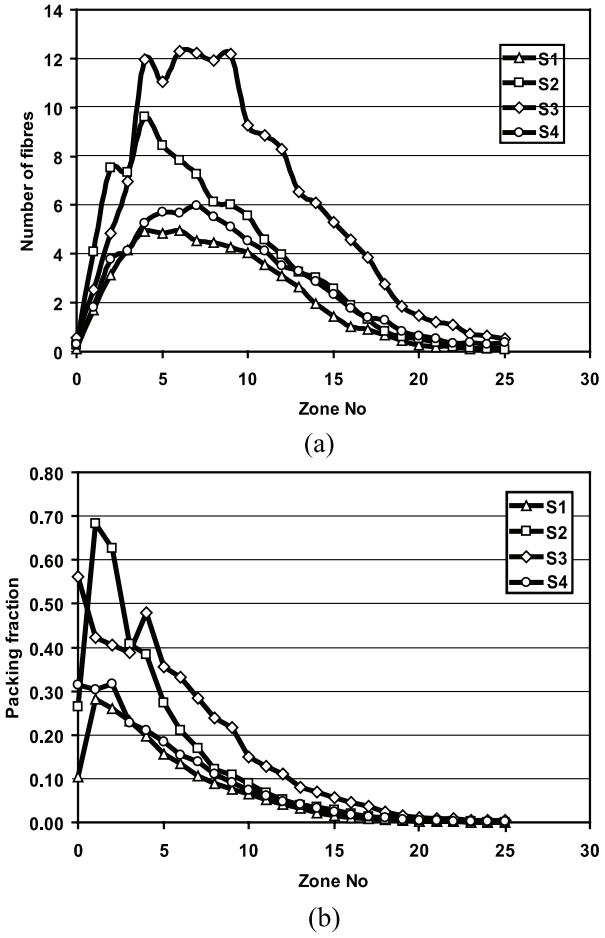

Figure 15 Predicted distributions: (a) the average number of fibers in ring zones; (b) fiber packing density in ring zones.

*S*4 and *S*1. It can be seen that for these samples the increase in the twist factor corresponds to the increase in twist angle, the decrease in the probability to remain in the zone, and, as a result, to a shorter migration distance. At the same time, the decrease in the probability to remain in the zone leads to the increase in the probabilities to migrate inwards and outwards.

The predicted total number of fibers agreed with the general tendency of a thicker yarn having a greater number of fibers in the cross-section. It was found that the accuracy in predicting the total number of fibers in the yarn cross-section very much depends on the twist factor of the yarn; see Figure 9(a) and Figure 15(a) and Table 7 where relative error was calculated as an absolute difference between the experimental and predicted number of fibers divided by the experimental value. The best result of 3.3 % difference

Table 7 Total number of fibers in the yarn cross-section.

Sample	Twist factor	Total number of fibers		Relative error, %
		Experimental	Predicted	
*S*1	158.1	91	58	36.3
*S*2	79.0	90	93	3.3
*S*3	118.5	190	150	21.0
*S*4	118.4	96	72	25.0

was achieved for sample *S*2 which has the lowest twist factor of 79.0.

This can be attributed to the fact that the experimentally-estimated migration probabilities used for resolving the system of linear equations, equation (8), were not unconditional probabilities. The migration behavior of a single fiber observed in the tracer-fiber experiment was affected by the presence of other fibers whose behavior could not be detected in the experiment. Thus, the estimated migration probabilities of a single migrating fiber were in fact the probabilities of migration patterns *A* to *D* in Figure 6 which involve more than one migrating fiber; this was discussed in the Estimation of the Number of Contact Points Between Fibers Due to Migration section. This in particular concerns the central zones which are densely populated with fibers and yarns with a high twist factor, e.g. sample *S*1 with the twist factor of 158.1 for which relative error was 36.3 %. Elementary migrations involving single fibers are most likely to occur in the outer zones and in yarns with a low twist factor where fibers have more freedom to migrate. Thus, it is reasonable to assume that the migration probabilities obtained for sample *S*2 were close estimates of unconditional probabilities required to resolve equation (8) resulting in a good prediction of fiber distribution in the yarn cross-section.

The same consideration with regards to migration probabilities applies to the distribution of the number of fibers in the ring zones (Figure 9(a) and Figure 15(a)) and the distribution of fiber packing fraction, which is based on the number of fibers (Figure 9(b) and Figure 15(b)). Generally, the predicted distributions in Figure 15(a) and (b) follow the same pattern as the experimental distributions, i.e. they show a more densely populated ring zones closer to the yarn axis with the thicker yarn (sample *S*3) having the greatest number of fibers in the zones and a gradually decreasing value towards the outer zones. The closest similarity between the experimental and predicted distributions of fiber packing fraction can be seen in sample *S*2 which has the lowest twist factor.

A better experimental technique is required that would enable the behavior of all fibers in the cross-section to be observed simultaneously. This can be achieved by studying a yarn in which all fibers are differently colored. Not only would it be practically difficult to make a yarn of this kind,

but it would also be difficult to distinguish fibers with inevitably small differences in color. For these reasons, a new approach for determining the migration probabilities is required; this will be considered in Part II.

Conclusion

This paper reports an attempt to use Jackson open network of $M/M/1$ queuing systems for modeling the fiber migration in staple fiber yarns. Every queuing system in the network describes the behavior of fibers with regards to an individual virtual location in the yarn cross-section. The model provides a detailed description of fiber migration in terms of migration probabilities, fiber arrival and termination rates, and migration distance. These parameters have a direct link with the yarn technical specification, including yarn and fiber linear density and fiber length. For example, the average number of fibers in the yarn cross-section, $\overline{N}$, can be estimated through average linear density of yarn, $\overline{T}_y$, and average linear density of fibers, $\overline{T}_f$, $\overline{N} = \overline{T}_y/\overline{T}_f$. Since the average number of fibers in the yarn cross-section is stable, the arrival rate of new fibers must be equal to the overall fiber termination rate. The total arrival rate of new fibers can be estimated as

$$\lambda^0 = \overline{N}/\overline{L}_f = \lambda_{00}^0 + \sum_{i=1}^{K-1} \sum_{r=0}^{|E_i|-1} \lambda_{ir}^0 , \qquad (22)$$

where $\overline{L}_f$ is average fiber length; λ_{ir}^0 is the arrival rate of new fibers for the VL r in zone i; K is the number of ring zones.

The total arrival rate corresponds to the distance between the leading-ends of the fibers which can be measured experimentally.

The model can be used for modeling a wide range of yarns with different structures. For example, assuming that migration probabilities $p_{ir;js}$ (see equation (7)) equal to 0 for all $i \neq j$ and for all r and s will lead to a yarn where fibers do not migrate at all; all fibers in such a yarn will follow perfect helices of a constant radius and pitch. Marl and mottle yarns can be modeled by assuming that $p_{ir;js} = 0$ for the virtual locations that are at both sides of a boundary dividing the yarn cross-section into two parts which are predominantly occupied by the fibers of a specific color. It is known that ring-spun and open-end spun yarns have different migration patterns [1, 28]; in particular, fibers in the open-end spun yarns tend to migrate less frequently than they do in the case of ring-spun yarn. In terms of the proposed model, this means that the probabilities to migrate inwards and outwards for the open-end yarn must be much lower in comparison with those for the ring-spun yarn. Yarns with a high level of hairiness can be modeled by assigning high probabilities to migrate outwards for the ring zones which are close to the yarn surface.

The model can be used for estimating the number of contact points between fibers in the yarn which is a very important characteristic for modeling the yarn mechanics.

In this paper, the migration probabilities have been obtained experimentally. However, the model provides a means for investigating the relationship between the migration probabilities, the arrival rates, and the distribution of fibers in the yarn cross-section via equations (8), (9), (11) and (13). These equations can be resolved in a direct order as has been shown above in the Experiments section or in inverse order using a suitable minimization algorithm, in which case the migration probability can be found given the distribution of the number of fibers in the yarn cross-section. This is considered in Part II of the series; in Part III this model is used to predict the color of melange yarns.

Acknowledgements

The work reported in this paper is a part of the joint research project between De Montfort University and the University of Leeds funded by the EPSRC grants GR/S77325/01 and GR/S77318/01. The authors would like to thank Mr E. J. Watson for preparing yarn cross-sections and digital images of tracer fibers.

Literature Cited

1. Hearle, J. W. S., Lord, P. R., and Senturk, N., Fibre Migration in Open-end-spun Yarns, *J. Textile Inst.* **63**, 605–617 (1972).
2. Truevtsev, N. N., Grishanov, S. A., and Harwood, R. J., The Development of Criteria for the Prediction of Yarn Behaviour Under Tension, *J. Textile Inst.* **88**, 400–414 (1997).
3. El-Sheikh, A., and Backer, S., The Mechanics of Fibre Migration. Part I: Theoretical Analysis, *Textile Res. J.* **42**(3), 137–146 (1972).
4. Gupta, B. S., Fibre Migration in Staple Yarns. Part II: The Geometric Mechanism of Fibre Migration and the Influence of the Roving and Drafting Variables, *Textile Res. J.* **40**(1), 15–24 (1970).
5. Hearle, J. W. S., and Bose, O. N., Migration of Fibres in Yarns. Part II: A Geometrical Explanation of Migration, *Textile Res. J.* **35**, 693–699 (1965).
6. Treloar, L. R. G., A Migrating-filament Theory of Yarn Properties, *J. Textile Inst.* **56**, T359–T380 (1965).
7. Neckar, B., Soni, M. K., and Das, D., Modelling of Radial Fiber Migration in Yarns, *Textile Res. J.* **76**(6), 486–491 (2006).
8. Tao, X., Mechanical Properties of a Migrating Fiber, *Textile Res. J.* **66**(12), 754–762 (1996).
9. Gupta, B. S., Fibre Migration in Staple Yarns. Part III: An Analysis of Migration Force and the Influence of the Variables in Yarn Structure, *Textile Res. J.* **42**(3), 181–196 (1972).
10. Abhiraman, A. S., and George, W., Fibre Migration as a Semimarkov Process, *Textile Res. J.* **44**(10), 736–738 (1974).
11. Kapitanov, A. F., Modelling Contacts Between Oriented Fibres, *Proc. Higher Sch. Technol. Textile Ind.* **10**, 23–28 (1992).

12. Morris, P. J., Merkin, J. H., and Rennell, R. W., Modelling of Yarn Properties from Fibre Properties, *J. Textile Inst.* **90**, 322–335 (1999).
13. Pan, N., Development of a Constitutive Theory for Short Fibre Yarns: Mechanics of Staple Yarn without Slippage Effect, *Textile Res. J.* **62**(10), 749–765 (1992).
14. Sreprateep, K., and Bohez, E. L. J., Computer Aided Modelling of Fiber Assemblies, *Comput. Aided Des. Appl.* **3**(1–4), 367–376 (2006).
15. Grishanov, S. A., Harwood, R. J., and Bradshaw, M. S., A Model of Fibre Migration in Staple-fibre Yarn, *J. Textile Inst.* **90**, 298–321 (1999).
16. Truevtsev, N. N., Legesina, G. I., Grishanov, S. A., and Asnis, L. M., Structural Features of Flax Blended Yarns, *Textile Ind.* **6**, 21–22 (1995).
17. Baskett, F., Chandy, K. M., Muntz, R. R., and Palacios, F. G., Open, Closed, and Mixed Networks of Queues with Different Classes of Customers, *J. Assoc. Comput. Mach.* **22**(2), 248–260 (1975).
18. Denning, P. J., and Buzen, J. P., The Operational Analysis of Queueing Network Models, *ACM Comput. Surv.* **10**(3), 225–261 (1978).
19. Hamilton, J. B., The Radial Distribution of Fibres in Blended Yarns, *J. Textile Inst.* **49**(9), T411–T423 (1958).
20. Oxtoby, E., "Spun Yarn Technology," Butterworths, London, UK (1987).
21. Pan, N., A Modified Analysis of the Microstructural Characteristics of General Fibre Assemblies, *Textile Res. J.* **63**, 336–345 (1993).
22. Komori, T., and Itoh, M., A Modified Theory of Fiber Contact in General Fiber Assemblies, *Textile Res. J.* **64**(9), 519–528 (1994).
23. Morton, W. E., and Yen, K. C., The Arrangement of Fibers in Fibro Yarns, *J. Textile Inst.* **43**(60) T60–T66 (1952).
24. Textiles – Standard Atmospheres for Conditioning and Testing, British Standard BS EN 20139:1992, British Standard Institution, London, UK, ISBN 0 580 20547 9 (1992).
25. Textiles – Determination of Twist in Yarns – Direct Counting Method, British Standard BS EN 2061:1996, British Standard Institution, London, UK, ISBN 0 580 25377 5 (1996).
26. Grishanov, S. A., Lomov, S. V., Cassidy, T., and Harwood, R. J., The Simulation of the Geometry of a Two-component Yarn. Part II: Fibre Distribution in the Yarn Cross-section, *J. Textile Inst.* **88**, 352–372 (1997).
27. Hickie, T. S., and Chaikin, M., Some Aspects of Worsted-yarn Structure. Part III: The Fibre-packing Density in the Cross-section of Some Worsted Yarns, *J. Textile Inst.* **65**, 433–437 (1974).
28. Truevtsev, N. N., "The Properties of Open-end Spun Yarn," Leningrad Institute of Technology, Leningrad, Russia (1977).